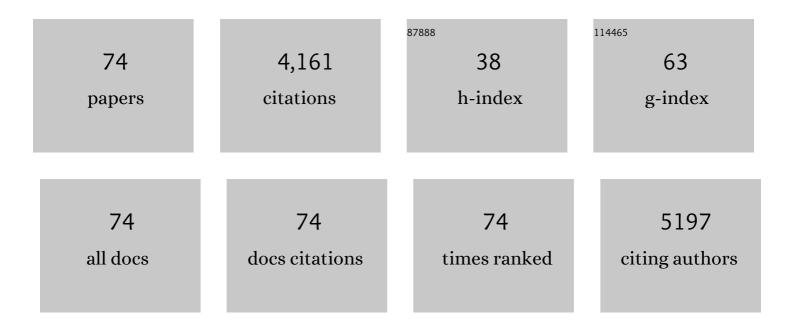
List of Publications by Year in descending order

Source: https://exaly.com/author-pdf/2371312/publications.pdf Version: 2024-02-01



#	Article	IF	CITATIONS
1	Selfâ€Healing Polymer Electrolyte for Dendriteâ€Free Li Metal Batteries with Ultraâ€Highâ€Voltage Niâ€Rich Layered Cathodes. Small, 2022, 18, e2200891.	10.0	23
2	Proof of Concept for Operando Infrared Spectroscopy Investigation of Light-Excited Metal Oxide-Based Gas Sensors. Journal of Physical Chemistry Letters, 2022, 13, 3631-3635.	4.6	2
3	A Pressure Responsive Artificial Interphase Layer of BaTiO <sub>3</sub> against Dendrite Growth for Stable Lithium Metal Anodes. Batteries and Supercaps, 2022, 5, .	4.7	3
4	A Bioâ€Inspired Neuromorphic Sensory System. Advanced Intelligent Systems, 2022, 4, .	6.1	18
5	Printable Zinc-Ion Hybrid Micro-Capacitors for Flexible Self-Powered Integrated Units. Nano-Micro Letters, 2021, 13, 19.	27.0	81
6	Inorganic Solid Electrolytes for Allâ€Solidâ€State Sodium Batteries: Fundamentals and Strategies for Battery Optimization. Advanced Functional Materials, 2021, 31, 2008165.	14.9	55
7	Hybrid electrolytes with an ultrahigh Li-ion transference number for lithium-metal batteries with fast and stable charge/discharge capability. Journal of Materials Chemistry A, 2021, 9, 18239-18246.	10.3	25
8	Integrated interface between composite electrolyte and cathode with low resistance enables ultra-long cycle-lifetime in solid-state lithium-metal batteries. Science China Chemistry, 2021, 64, 673-680.	8.2	16
9	Memristive Devices with Multiple Resistance States Based on the Migration of Protons in αâ€MoO <sub>3</sub> /SrCoO <sub>2.5</sub> Stacks. Advanced Electronic Materials, 2021, 7, 2001243.	5.1	5
10	Ultravioletâ€Cured Semiâ€Interpenetrating Network Polymer Electrolytes for Highâ€Performance Quasiâ€Solidâ€State Lithium Metal Batteries. Chemistry - A European Journal, 2021, 27, 7773-7780.	3.3	8
11	An artificial olfactory inference system based on memristive devices. InformaÄnÃ-Materiály, 2021, 3, 804-813.	17.3	50
12	Light-excited chemiresistive sensors integrated on LED microchips. Journal of Materials Chemistry A, 2021, 9, 16545-16553.	10.3	7
13	Multi-gate memristive synapses realized with the lateral heterostructure of 2D WSe <sub>2</sub> and WO <sub>3</sub> . Nanoscale, 2020, 12, 380-387.	5.6	47
14	Flexible and transparent sensors for ultra-low NO <sub>2</sub> detection at room temperature under visible light illumination. Journal of Materials Chemistry A, 2020, 8, 14482-14490.	10.3	39
15	Artificial Intelligence to Power the Future of Materials Science and Engineering. Advanced Intelligent Systems, 2020, 2, 2070042.	6.1	3
16	Artificial Intelligence to Power the Future of Materials Science and Engineering. Advanced Intelligent Systems, 2020, 2, 1900143.	6.1	75
17	Electroformingâ€Free Artificial Synapses Based on Proton Conduction in αâ€MoO 3 Films. Advanced Electronic Materials, 2020, 6, 1901290.	5.1	14
18	<i>In situ</i> thermally polymerized solid composite electrolytes with a broad electrochemical window for all-solid-state lithium metal batteries. Journal of Materials Chemistry A, 2020, 8, 3892-3900.	10.3	59

#	Article	IF	CITATIONS
19	Artificial Neural Networks Based on Memristive Devices: From Device to System. Advanced Intelligent Systems, 2020, 2, 2000149.	6.1	39
20	A New Lithiumâ€Ion Conductor LiTaSiO <sub>5</sub> : Theoretical Prediction, Materials Synthesis, and Ionic Conductivity. Advanced Functional Materials, 2019, 29, 1904232.	14.9	15
21	Three-Dimensional Garnet Framework-Reinforced Solid Composite Electrolytes with High Lithium-Ion Conductivity and Excellent Stability. ACS Applied Materials & Interfaces, 2019, 11, 26920-26927.	8.0	87
22	Solid Electrolytes: A New Lithiumâ€lon Conductor LiTaSiO <sub>5</sub> : Theoretical Prediction, Materials Synthesis, and Ionic Conductivity (Adv. Funct. Mater. 37/2019). Advanced Functional Materials, 2019, 29, 1970253.	14.9	4
23	MOF-derived nanoporous multifunctional fillers enhancing the performances of polymer electrolytes for solid-state lithium batteries. Journal of Materials Chemistry A, 2019, 7, 2653-2659.	10.3	160
24	Hierarchically-structured MnFe2O4 nanospheres for highly sensitive detection of NO2. Solid State lonics, 2019, 336, 102-109.	2.7	11
25	Silverâ€Quantumâ€Dotâ€Modified MoO <sub>3</sub> and MnO <sub>2</sub> Paperâ€Like Freestanding Films f Flexible Solidâ€State Asymmetric Supercapacitors. Small, 2019, 15, e1805235.	or 10.0	79
26	Structure and magnetic properties of highly oriented LaBaCo2O5+Î′ films deposited on Si wafers with Pt/Ti buffer layer. Physical Chemistry Chemical Physics, 2019, 21, 22390-22395.	2.8	1
27	Quasiâ€Hodgkin–Huxley Neurons with Leaky Integrateâ€andâ€Fire Functions Physically Realized with Memristive Devices. Advanced Materials, 2019, 31, e1803849.	21.0	87
28	Artificial Neurons: Quasiâ€Hodgkin–Huxley Neurons with Leaky Integrateâ€andâ€Fire Functions Physically Realized with Memristive Devices (Adv. Mater. 3/2019). Advanced Materials, 2019, 31, 1970020.	21.0	0
29	Bienenstock, Cooper, and Munro Learning Rules Realized in Secondâ€Order Memristors with Tunable Forgetting Rate. Advanced Functional Materials, 2019, 29, 1807316.	14.9	60
30	Nanostructured Metal–Organic Framework (MOF)â€Derived Solid Electrolytes Realizing Fast Lithium Ion Transportation Kinetics in Solid‣tate Batteries. Small, 2019, 15, e1804413.	10.0	93
31	In Situ Formed Shields Enabling Li <sub>2</sub> CO <sub>3</sub> -Free Solid Electrolytes: A New Route to Uncover the Intrinsic Lithiophilicity of Garnet Electrolytes for Dendrite-Free Li-Metal Batteries. ACS Applied Materials & Interfaces, 2019, 11, 898-905.	8.0	147
32	LaFeO3 porous hollow micro-spindles for NO2 sensing. Ceramics International, 2019, 45, 5240-5248.	4.8	25
33	Photonic Potentiation and Electric Habituation in Ultrathin Memristive Synapses Based on Monolayer MoS <sub>2</sub> . Small, 2018, 14, e1800079.	10.0	224
34	Memristive Synapses with Photoelectric Plasticity Realized in ZnO <sub>1–<i>x</i></sub> /AlO <sub><i>y</i></sub> Heterojunction. ACS Applied Materials & Interfaces, 2018, 10, 6463-6470.	8.0	120
35	NO2 sensing properties of SmFeO3 porous hollow microspheres. Sensors and Actuators B: Chemical, 2018, 265, 443-451.	7.8	41
36	Synaptic Suppression Triplet‧TDP Learning Rule Realized in Secondâ€Order Memristors. Advanced Functional Materials, 2018, 28, 1704455.	14.9	183

#	Article	IF	CITATIONS
37	Detecting low concentration of H2S gas by BaTiO3 nanoparticle-based sensors. Sensors and Actuators B: Chemical, 2017, 238, 16-23.	7.8	48
38	Molybdenum trioxide nanopaper as a dual gas sensor for detecting trimethylamine and hydrogen sulfide. RSC Advances, 2017, 7, 3680-3685.	3.6	52
39	Electrospun Ni-doped SnO2 nanofiber array for selective sensing of NO2. Sensors and Actuators B: Chemical, 2017, 244, 509-521.	7.8	72
40	Origin of the low grain boundary conductivity in lithium ion conducting perovskites: Li <sub>3x</sub> La <sub>0.67â^'x</sub> TiO <sub>3</sub> . Physical Chemistry Chemical Physics, 2017, 19, 5880-5887.	2.8	100
41	Hierarchical flowerlike WO3 nanostructures assembled by porous nanoflakes for enhanced NO gas sensing. Sensors and Actuators B: Chemical, 2017, 246, 225-234.	7.8	57
42	Characteristics and sensing properties of CO gas sensors based on LaCo 1â^'x Fe x O 3 nanoparticles. Solid State Ionics, 2017, 303, 97-102.	2.7	19
43	Single crystalline SrTiO3 as memristive model system: From materials science to neurological and psychological functions. Journal of Electroceramics, 2017, 39, 210-222.	2.0	14
44	Pavlovian conditioning demonstrated with neuromorphic memristive devices. Scientific Reports, 2017, 7, 713.	3.3	49
45	Garnet-Type Fast Li-Ion Conductors with High Ionic Conductivities for All-Solid-State Batteries. ACS Applied Materials & Interfaces, 2017, 9, 12461-12468.	8.0	179
46	Gallium-Doped Li <sub>7</sub> La <sub>3</sub> Zr <sub>2</sub> O <sub>12</sub> Garnet-Type Electrolytes with High Lithium-Ion Conductivity. ACS Applied Materials & Interfaces, 2017, 9, 1542-1552.	8.0	266
47	Behavioral Plasticity Emulated with Lithium Lanthanum Titanateâ€Based Memristive Devices: Habituation. Advanced Electronic Materials, 2017, 3, 1700046.	5.1	19
48	Hierarchical and Hollow Fe <sub>2</sub> O <sub>3</sub> Nanoboxes Derived from Metal–Organic Frameworks with Excellent Sensitivity to H <sub>2</sub> S. ACS Applied Materials & Interfaces, 2017, 9, 29669-29676.	8.0	118
49	Bio-inspired high-performance solid-state supercapacitors with the electrolyte, separator, binder and electrodes entirely from <i>kelp</i> . Journal of Materials Chemistry A, 2017, 5, 25282-25292.	10.3	85
50	Hierarchical porous microspheres of activated carbon with a high surface area from spores for electrochemical double-layer capacitors. Journal of Materials Chemistry A, 2016, 4, 15968-15979.	10.3	80
51	3D Porous Hierarchical Microspheres of Activated Carbon from Nature through Nanotechnology for Electrochemical Double-Layer Capacitors. ACS Sustainable Chemistry and Engineering, 2016, 4, 6463-6472.	6.7	51
52	Mimicking the brain functions of learning, forgetting and explicit/implicit memories with SrTiO <sub>3</sub> -based memristive devices. Physical Chemistry Chemical Physics, 2016, 18, 31796-31802.	2.8	36
53	Synaptic Metaplasticity Realized in Oxide Memristive Devices. Advanced Materials, 2016, 28, 377-384.	21.0	210
54	Single crystalline flowerlike α-MoO3 nanorods and their application as anode material for lithium-ion batteries. Journal of Alloys and Compounds, 2016, 687, 79-86.	5.5	44

#	Article	IF	CITATIONS
55	Lotus pollen derived 3-dimensional hierarchically porous NiO microspheres for NO2 gas sensing. Sensors and Actuators B: Chemical, 2016, 227, 554-560.	7.8	77
56	Near room temperature CO sensing by mesoporous LaCoO3 nanowires functionalized with Pd nanodots. Sensors and Actuators B: Chemical, 2016, 222, 517-524.	7.8	44
57	Oxygen pump based on stabilized zirconia. Review of Scientific Instruments, 2015, 86, 115103.	1.3	9
58	SrTi0.65Fe0.35O3 nanofibers for oxygen sensing. Solid State Ionics, 2015, 278, 26-31.	2.7	11
59	NO sensing by single crystalline WO3 nanowires. Sensors and Actuators B: Chemical, 2015, 219, 346-353.	7.8	110
60	CO sensing mechanism of LaCoO3. Solid State Ionics, 2015, 272, 155-159.	2.7	17
61	Bio-templated fabrication of hierarchically porous WO <sub>3</sub> microspheres from lotus pollens for NO gas sensing at low temperatures. RSC Advances, 2015, 5, 29428-29432.	3.6	31
62	LaCoO <sub>3</sub> -based sensors with high sensitivity to carbon monoxide. RSC Advances, 2015, 5, 65668-65673.	3.6	31
63	Gigantically enhanced NO sensing properties of WO3/SnO2 double layer sensors with Pd decoration. Sensors and Actuators B: Chemical, 2015, 220, 398-405.	7.8	40
64	Effects of potassium iodide (KI) on crystallinity, thermal stability, and electrical properties of polymer blend electrolytes (PVC/PEO:KI). Solid State Ionics, 2015, 278, 260-267.	2.7	57
65	Oxygen sensors based on SrTi0.65Fe0.35O3â~`î´ thick film with MgO diffusion barrier for automotive emission control. Sensors and Actuators B: Chemical, 2015, 213, 102-110.	7.8	19
66	Ultraviolet photocatalytic degradation of methyl orange by nanostructured TiO <sub>2</sub> /ZnO heterojunctions. Journal of Materials Chemistry A, 2015, 3, 6565-6574.	10.3	141
67	Morphology engineering of nanostructured TiO <sub>2</sub> particles. RSC Advances, 2015, 5, 6481-6488.	3.6	5
68	Synthesis and characterization of one-dimensional metal oxides: TiO2, CeO2, Y2O3-stabilized ZrO2 and SrTiO3. Ceramics International, 2015, 41, 533-545.	4.8	13
69	Insulator-to-semiconductor transition of nanocrystalline BaTiO <sub>3</sub> at temperatures â‰⊉00 °C. Physical Chemistry Chemical Physics, 2014, 16, 20420-20423.	2.8	6
70	Cadmium removal in waste water by nanostructured TiO <sub>2</sub> particles. Journal of Materials Chemistry A, 2014, 2, 13932-13941.	10.3	37
71	Determination of electronic and ionic partial conductivities of a grain boundary: method and application to acceptor-doped SrTiO3. Solid State Ionics, 2002, 154-155, 563-569.	2.7	27
72	Defect Structure Modification in Zirconia by Alumina. Physica Status Solidi A, 2001, 183, 261-271.	1.7	22

#	Article	lF	CITATIONS
73	Hydrothermal degradation mechanism of tetragonal Zirconia. Journal of Materials Science, 2001, 36, 3737-3744.	3.7	59
74	Singleâ€lon Magnetostriction in Gd 2 O 3 –CeO 2 Solid Solutions. Advanced Functional Materials, 0, , 2110509.	14.9	0